

ISCI, Volume 15

Supplemental Information

Sodium Doping Pushes the Efficiency

of Carbon-Based CsPbI₃

Perovskite Solar Cells to 10.7%

Sisi Xiang, Weiping Li, Ya Wei, Jiaming Liu, Huicong Liu, Liqun Zhu, Shihe Yang, and Haining Chen

Transparent Methods

Preparation of TiO₂ mesoporous scaffolds. Firstly, TiO₂ blocking layer was spin-coated on cleaned FTO glass at 2000 rpm for 20 s using 0.15 M titanium diisopropoxide bis(acetylacetonate) in 1-butanol solution, followed by heating at 125 °C for 5 min. Then, TiO₂ films were deposited by spin coating at 5000 rpm for 30 s using a commercial TiO₂ paste (Dyesol 30 NRD, Dyesol) diluted in ethanol with a ratio of 1:2.5. After drying at 100 °C for 5 min, the TiO₂ films were gradually heated to 550 °C, baked at this temperature for 30 min and cooled to room temperature.

Deposition of CsPbI₃ and Cs_{1-x}Na_xPbI₃ films. DMF·HI·PbI₂ powder was prepared as introduced in our previous work^[6]. mixing 5 g PbI₂ and 4 ml HI in DMF and stirring overnight to ensure complete conversion. Light yellow DMF·HI·PbI₂ precipitates were obtained by pouring abundant ethanol into the above solution, followed by washing the precursor in ethanol for several times. The precipitates were filtered and dried in a vacuum oven at 60 °C for 2 h. CsPbI₃ films were deposited by one-step deposition method. The CsPbI₃ precursor solution was prepared by dissolving 1 M DMF·HI·PbI₂ and 1M CsI in DMF solvent at room temperature. The solution was spin-coated on the substrates that had been preheated to 70 °C at 2000 rpm for 20 s. Then, the samples were annealed at 200 °C for around 5 min to get CsPbI₃ films. For the Cs_{1-x}Na_xPbI₃ films, the whole procedure was similar except replacing xM CsI with NaI in the precursor solution.

Deposition of carbon electrode. A commercial carbon paste purchased from Guangzhou Seaside Technology Co., Ltd was used as carbon paint for carbon electrode. The carbon extraction layer was simply deposited by printing the carbon paint on CsPbI₃ films at room temperature, followed by heating at 120 °C for 30 min.

Films characterizations. X-ray diffraction (XRD) patterns were recorded on a Philips PW-1830 X-ray diffractometer with Cu K α radiation ($\lambda = 0.15418$ nm). TOF-SIMS was used to detect distribution of different elements, collected in the positive ion detection mode employing 30 keV Bi⁺ primary beam with a diameter of 100 μ m and recorded on TOF.SIMS 5-100. The beam was at an angle of 45° with respect to the sample surface normal. Morphology was evaluated on a JEOL 6700F or 7100F SEM at an accelerating voltage of 5 kV. UV-vis absorption spectra were recorded on a Perkin-Elmer UV-vis spectrophotometer (model Lambda 20). Steady state PL spectra were measured on a Jobin Yvon (Laboratory RAM HR800) confocal micro-Raman spectrometer. Time resolved PL measurement was carried out on an ultrafast lifetime Spectrofluorometer (Delta flex) and a 475 nm ultrafast laser was used as the excitation light source. Fluorescence lifetime images were recorded on a laser scanning confocal microscope (A1R-si). Chemical states of film surface were evaluated by an X-ray photoemission spectroscopy (XPS, ESCALab250Xi). The energy positions were recorded on an ultraviolet photoelectron spectroscopy (UPS, ESCALab250Xi).

Photovoltaic characterizations. The solar light simulator (Newport Oriel Sol3A, model number 94063A, AM 1.5 global filter) was calibrated to 1 sun (100 mW/cm²) using an Oriel reference solar cell (monocrystalline silicon) and meter. The active cell area was all fixed at about 6.25 mm² using a metal mask. Each ten cells were used to collect the relevant cell parameters of different doping amount in Figure 2(b)-(e). J-V curves and intensity modulated photocurrent/photovoltage spectroscopy (IMPS/IMVS) and open-circuit voltage decay (OCVD) measurement were recorded

on a ZENNIUM pro electrochemical workstation (ZAHNER-Elektrik GmbH & Co., KG, Germany). The wavelength of the irradiation light for IMPVS and OCVD measurement is 417 nm. IPCE spectra were recorded using IPCE kit (E0201, Institute of Physics, Chinese Academy of Sciences) in AC mode.

Stability evaluation. The device stability was studied by storing the device under room temperature (20-30 °C) in air atmosphere with a humidity lower than 30 %. J-V curves were measured periodically in ambient air (about 30-80 % humidity) to get the photovoltaic parameters. The photostability was tested under continuous one-sun illumination (100 mW/cm^{-2}) at RT and 65 °C in ambient atmosphere without encapsulation (humidity~40%).

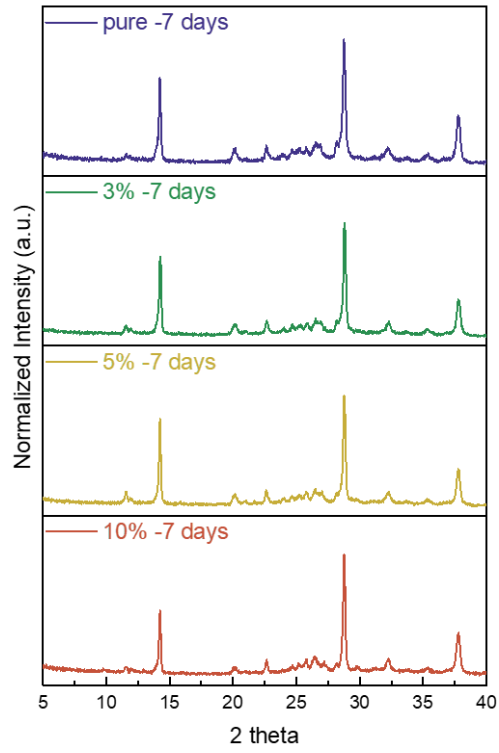
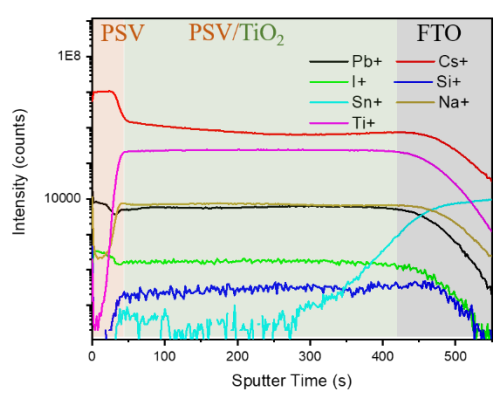
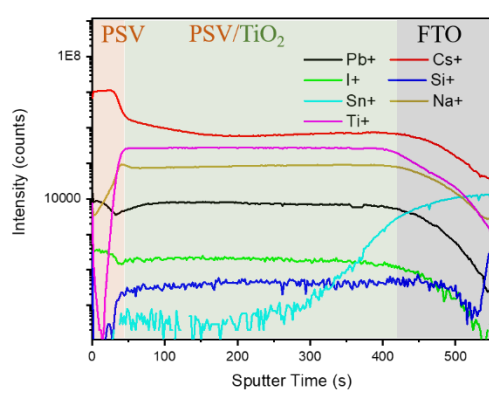


Figure S1. XRD patterns of the CsPbI₃ perovskite films with different Na doping concentrations after 7 days storage in air atmosphere (20-35 °C and 10-20% humidity). Related to Figure 1(a).



pure



Na-doped

Figure S2. SIMS depth profile for Cs, Pb, I, Na, Sn, Si and Ti elements in CsPbI_3 and $\text{Cs}_{0.95}\text{Na}_{0.05}\text{PbI}_3$ films. Related to Figure 1(c).

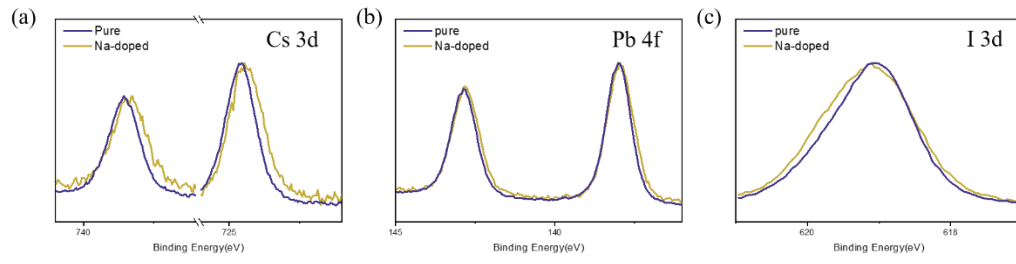


Figure S3. Comparison of high-resolution XPS spectra of the CsPbI₃ and Cs_{0.95}Na_{0.05}PbI₃ films: (a) Cs 3d. (b) Pb 4f. (c) I 3d. Related to Figure 1(d).

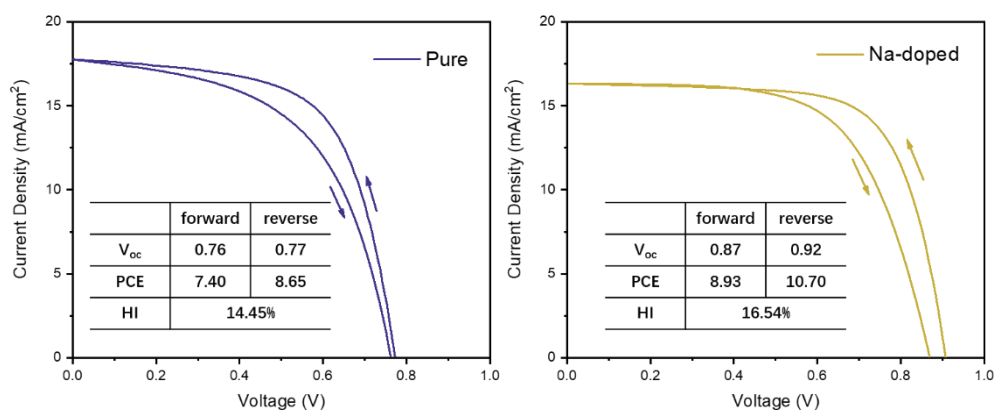


Figure S4. J-V curves obtained from different scan directions of CsPbI₃ and Cs_{0.95}Na_{0.05}PbI₃C-PSCs. Insets are the cell parameters obtained from different scan directions. Related to Figure 3.

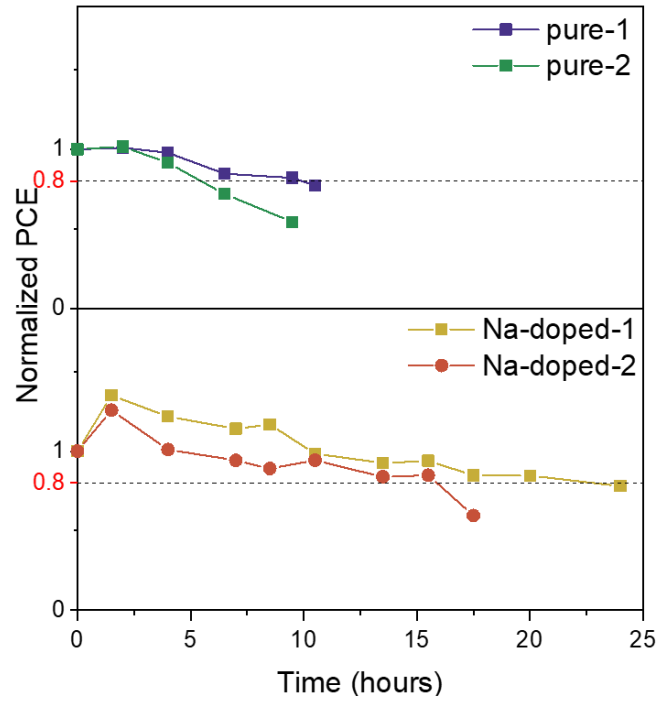


Figure S5. Photostability measurement of the devices under continuous one-sun illumination (100 mW/cm^{-2}) in ambient atmosphere without encapsulation (room temperature (about $20 \text{ }^{\circ}\text{C}$) and humidity~40%). Related to Figure 3.

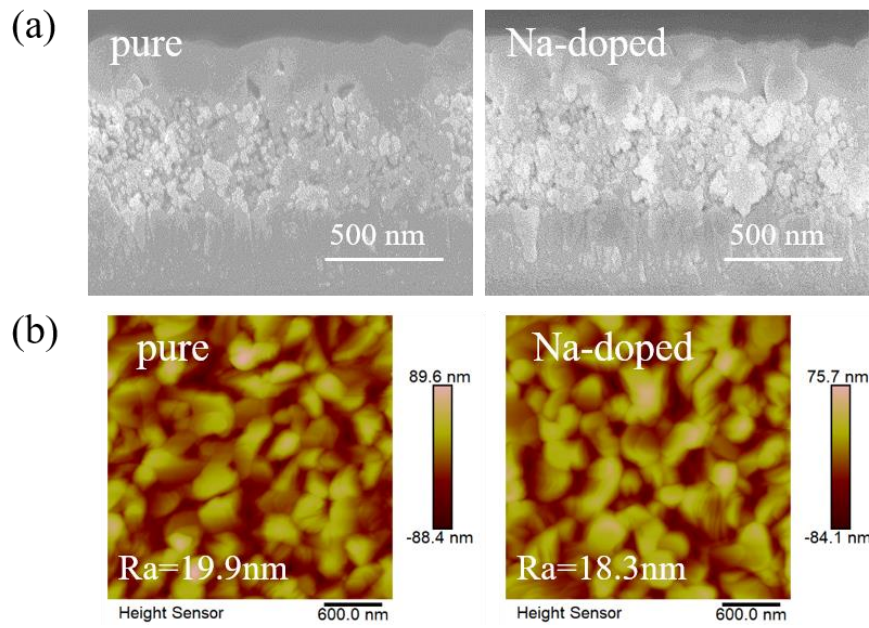


Figure S6. Morphology of CsPbI_3 and $\text{Cs}_{0.95}\text{Na}_{0.05}\text{PbI}_3$ films. (a) Cross-sectional SEM images (b) AFM images. Related to Figure 3 and 4.

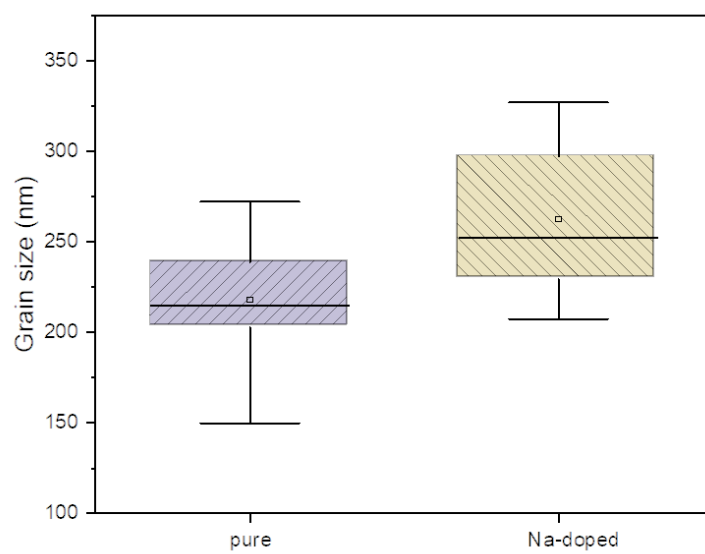


Figure S7. Grain size distribution of CsPbI_3 and $\text{Cs}_{0.95}\text{Na}_{0.05}\text{PbI}_3$ films. Related to Figure 4.

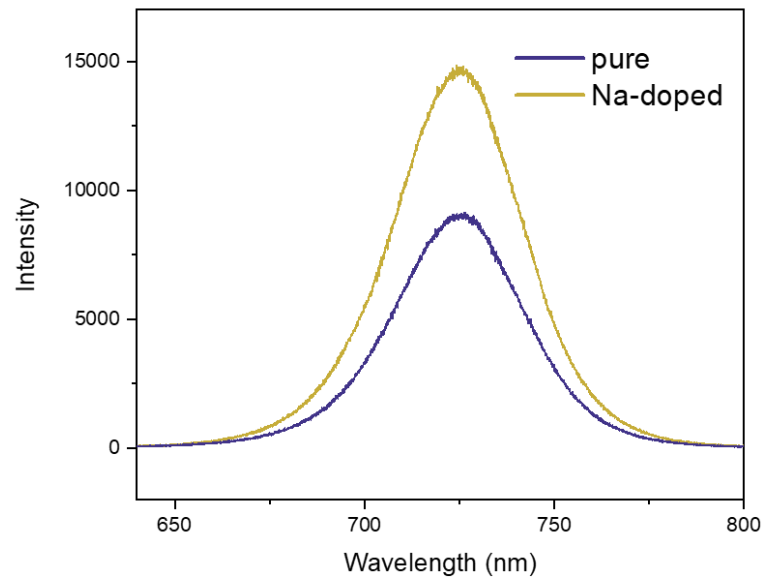


Figure S8. Steady-state PL of CsPbI₃ and Cs_{0.95}Na_{0.05}PbI₃ films. Related to Figure 4.

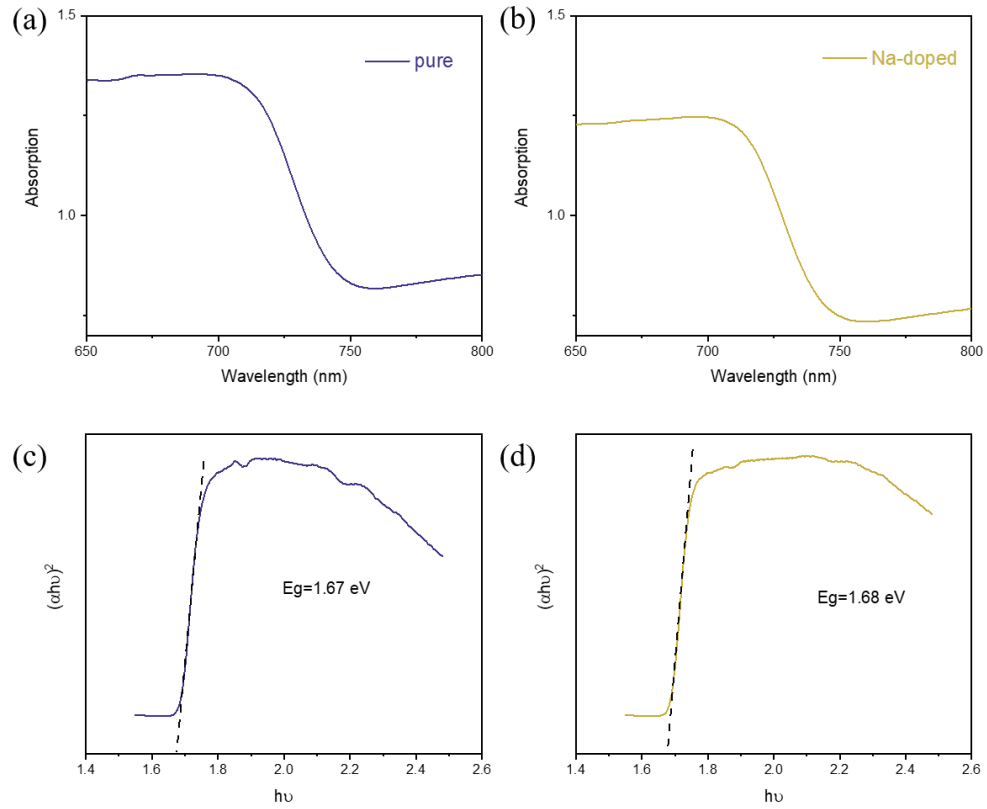


Figure S9. UV-vis spectra of (a) CsPbI₃ and (b) Cs_{0.95}Na_{0.05}PbI₃ films. $(\alpha h\nu)^2$ vs $h\nu$ curves of (c) CsPbI₃ and (d) Cs_{0.95}Na_{0.05}PbI₃ films. Related to Figure 4.

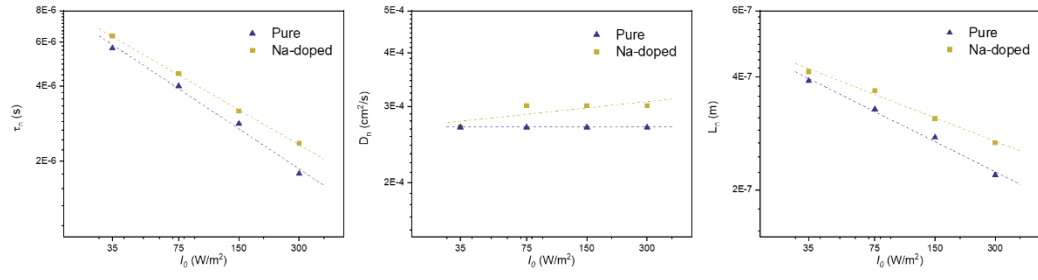


Figure S10. (a) Electron lifetime (τ_n), (b) electron diffusion coefficients (D_n) and (c) diffusion length (L_n) as a function of light density (I_0) for CsPbI₃ and Cs_{0.95}Na_{0.05}PbI₃ C-PSCs. Related to Figure 5.